Determination of the solicitation types responsible for the deformed shape of an aircraft cockpit

Infante, V.[1*], Gomes, E. [1] and Branco, C.M. [1]

[1] Departamento de Engenharia Mecânica, Instituto Superior Técnico

Av. Rovisco Pais, 1096 Lisboa Codex

* Corresponding autor. Tel.: +351 21 8417643; fax: +351 21 8417915

E-mail address: virginia@dem.ist.utl.pt

Abstract:

During the last decade, some studies have been done, concerning the evaluation of aeronautical components in terms of the load conditions applied to cockpit geometries.

The present study aims to determine the solicitation types which could be responsible for the deformed shape of an aircraft cockpit after an accident. Experimental tests were carried out in order to obtain the deformed geometries of the different structural supporting components.

Using CAD software (CATIA and SOLIDWORKS) together with a 3D scanner, a 3D modelation was obtained, from an undeformed aircraft cockpit.

Due to the complexity of the shape of the cockpit, a finite element approach was adopted and the components were modeled and analysed for a series of representative load cases in order to find out the most likely solicitations compatible with a deformed shape of the cockpit´s structure. The 3D model of the cockpit, obtained with the CAD software, was analysed with the finite element programs ABAQUS and ANSYS. The result and outcomes are presented herein.

A experimental specimen was modeled and analysed by FE program in order to validate the results obtained for the cockpit modelation.

In addition some guidance is given on the verification of the solicitation which could be responsible for the deformed shape of an aircraft cockpit.

1. Introduction

Aviation accident law covers both major air carrier and general aviation accidents. General aviation includes all non-commercial aircraft including small planes, large business jets, charter flights, pleasure crafts, helicopters, and hang gliders. The most common causes of both major carrier and general aviation accidents include [1]:

- Pilot error
- Other Human Error
- Weather
- Mechanical Failure
- Sabotage
- Other causes

The analysis of the accidents helps identifying the elements that affect aviation conditions, the relationships between them, and how they may contribute to the occurrence of dangerous situations.

In this paper the authors present several Finite Element analysis to determine the solicitation types which could be responsible for the deformed shape of an aircraft cockpit after an accident. These solicitation types represent different causes of failures such as fire, midair collision, and in-flight explosion.

This study was carried out on the cockpit of a non-commercial small plane. Using different solicitations, the cockpit deformations were computed with the 3D FE programs.

In order to obtain a comparison between the numerical analysis and the experimental data, a numerical simulation was performed on a specimen obtained from the cockpit. This specimen was then subjected to experimental tests.

The outline applied was:

The Cockpit´s geometry was modeled using 3D geometry modeling programs such as CATIA and SOLIDWORKS.

The specimen geometry was based on the cockpit modelation (Figure 1).

A mechanical characterization of the different materials was made for input in the FE analysis program.

The 3D mesh applied to the models was optimized for the convergence of results and for the element type selection.

The study and selection of the boundary and load conditions was performed. On the cockpit model were simulated different loads conditions which could occur and act on the cockpit during an accident.

With the obtained results a comparative analysis was performed between the experimental and the computed deformations.

For the modelations the finite element commercial codes ANSYS (version 8.0) [2] and ABAQUS (version 6.5) [3] were used. The hardware was a PC, Pentium 4 – 3GHz processor with 1.5 GB of RAM.

2. Cockpit and specimen modelation

Due to the complexity of the cockpit geometry the model includes only the windscreen and the direct support structure.

The windscreen is composed by acrylic glass (PMMA), aluminum alloy 2024TB plate in the exterior zone and aluminum profiles in the interior zone, connected by stainless steel bolts.

The following simplifications were assumed for the cockpit and for the specimen simulation:

- The materials were considered homogeneous and isotropic
- Symmetry was maintained for the cockpit by imposing the appropriate displacement constraints

To obtain the geometric shape of the cockpit, the following steps were performed:

- Drawing of a mesh on the cockpit acrylic surface using an acetate pen (Figure 1)
- Find, using a 3D Scanner robot harm (fabrication SARO), and register (with the Rhinocerus cad software), the different mesh points (drawn in the last step).
- Transfer all the measured points to the CATIA drawing program.

- Creation of the 3D geometric model for the acrylic glass using the CATIA program (Figure 2)
- Creation of the 3D geometric model for the plates and profiles using the SOLIDWORKS drawing program (Figure 3)
- Final geometries importation to the Finite Element code ANSYS

The options for the different drawing programs are based in the geometric complexity of the components to model.

2.1 Cockpit and specimen geometries importation and reconstruction using the ANSYS program

After the construction and importation of the cockpit geometric models to the ANSYS Finite Element program it was crucial to reconstruct all areas and volumes.

Figure 4 is a photograph of the cockpit set reconstructed by ANSYS program. It can be stated that the geometries obtained in the ANSYS program are very similar to the ones drawn with the CAD geometric modelers.

After the cockpit geometry reconstruction made using the ANSYS code, the different volumes so obtained were exported in IGES format to the ABAQUS program for the FE analysis.

2.2 Meshing, boundary and load conditions applied to the specimen

Ten-noded isoparametric, tridimensional and tetrahedral elements (C3D4) were used to mesh the specimen.

Table 1 shows the number of nodes, elements and degrees of freedom used.

Specimen mesh as shown in figure 5. Most of the significant geometric features were modeled and a relatively finer mesh was used for the bolts connections region. The global mesh density was chosen to minimize discretisation errors.

Essential boundary condition applied to the specimen element prescribed the Aluminum profile fixed edge (Figure 6).

Four concentrated loads with 130N which were applied in the specimen edge (Figure 7) to simulate the 520 N correspondent of the bending test load.

2.3 Meshing, boundary and load conditions applied to the cockpit

The same element type used on the specimen was applied to the cockpit model.

Table 2 shows the number of nodes, elements and degrees of freedom.

Figure 8 shows the cockpit set mesh.

As with the numerical model for the experimental specimen, the mesh was constructed to minimize the number of the distorted elements (aspect ratio).

The boundary conditions assumed in the cockpit simulations were the constraint of (Figure 9):

1. u displacement in x direction applied to the plate and U profile zone;
2. u displacement in x direction applied to the I profile end zone;
3. v and w displacements in y and z directions applied to the superior I profile zone;
4. w displacement in z direction applied to the bolts nuts;
5. v and w displacements in y and z directions applied to the U profile center.

The first boundary condition is specified by the cockpit symmetry.

The load conditions applied for the cockpit simulations were (Figure 10):

- Axial uniform distribute pressure applied in the interior cockpit zone;
- Axial uniform distribute pressure applied in the external cockpit zone;
- Axial uniform distribute pressure applied in 4 acrylic glass elements located in the central cockpit zone;
- Axial uniform distribute pressure applied in 4 acrylic glass elements located in the superior cockpit zone;
- Concentrated loads applied in cockpit inferior edge to simulate the aircraft noise flow impact.

Thermal effects were not taken in account in the simulations that were carried out.

2.4 Mechanical properties of the acrylic glass and aluminum

The materials mechanical properties, used in the Finite Element simulations were:

Acrylic glass:	Aluminum (plate and profiles):	Steel (bolts):
$\nu = 0.37$	$\nu = 0.3$	$\nu = 0.3$
E = 3.8 GPa	E = 73 GPa	E = 210 GPa
σ_{yield} = 79 MPa	σ_{yield} = 325 MPa	

2.5 Numeric results analysis of the specimen

The failure modus and the material deformation obtained in the bending tests are in concordance with the numerical analysis of the specimen.

In Figure 11 the deformed results obtained in the bending experimental specimen simulation are presented. The deformation obtained is qualitatively similar to the bending test.

The close failure stress values were obtained in the aluminum plate near the bolt connections zone. Therefore the material failure will initiate in the aluminum plate earlier than the acrylic glass rupture.

2.6 Numeric results analysis of the cockpit

Figure 12 a) shows the cockpit deformation mesh when a uniform interior pressure was applied. These results show a high deformation in the superior support plate. The material failure initiate in bolt connections zone considering the mechanical properties of the acrylic glass and aluminum.

The results obtained for the external uniform distributed pressure load (Figure 12 b)) shows a deformation from outside to inside, as was expected.

The degree of deformation obtained for an internal uniform distributed pressure in central zone of the cockpit is uniform in all the plate of the windscreen support (Figure 12 c)). Analyzing the cockpit stress distribution it is verified that the tearing of the Aluminum plate is uniform in all the screwed linking.

For an Internal uniform distributed pressure in superior zone of the cockpit the deformed shape obtained is more accented in the upper zone of the windscreen support (Figure 12 d)), verifying a smooth deformation in the inferior zone of cockpit.

The deformation obtained for concentrated loads applied to the inferior border of the cockpit windscreen is located in the upper zone of the cockpit where the concentrated loads are applied (Figure 12 e)). The stress distribution analysis shows that the set failure occurs in the acrylic glass.

3. Conclusions

- The specimen modelation has shown that the set initial failure is in aluminum plate, bolt connections zone, considering the boundary and loads conditions applied. The failure modus and the material deformation obtained in the bending tests are in concordance with the numerical analysis of the specimen.
- Comparing the numerical deformations presented in this paper with the deformed shape of a cockpit after an accident it is possible to predict the solicitation which is responsible for that shape.

4. References

[1] PlaneCrashInfo.com, http://www.planecrashinfo.com/cause.htm.

[2] ANSYS manuals, Ansys 8.0 Documentation, SAS, IP Inc 2004.

[3] ABAQUS/Standard User's Manual", version 6.5, Vol I, II e III; Hibbitt, Karlsson & Sorensen, Inc; 2001.

Table 1 – Meshes used for the computation in the specimen.

Number of nodes	**Number of elements**	**Number of DOF**
14682	50832	44046

Table 2 – Meshes used for the numerical simulation of the cockpit.

Number of nodes	Number of elements	Number of DOF
107894	312085	323682

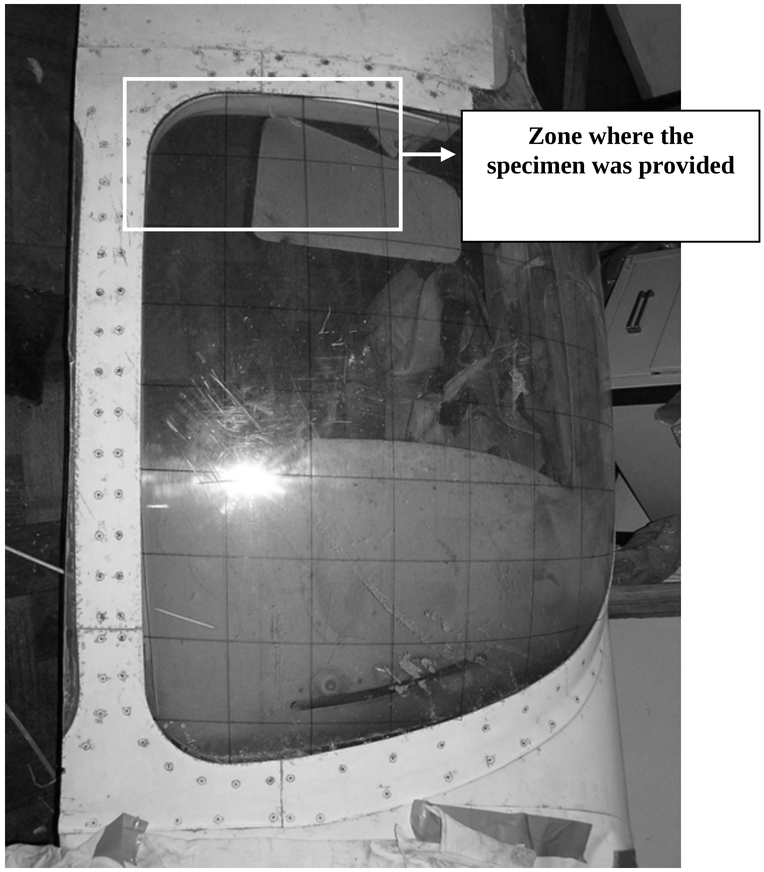

Figure 1 – Cockpit zone where the specimen was provided.

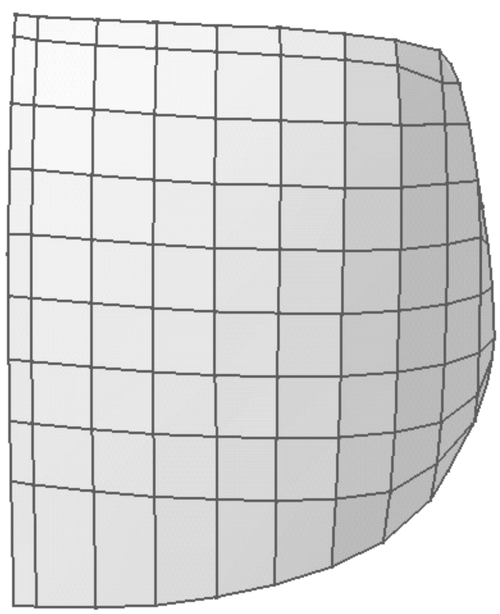

Figure 2 – Acrylic glass geometry obtained by CATIA drawing program.

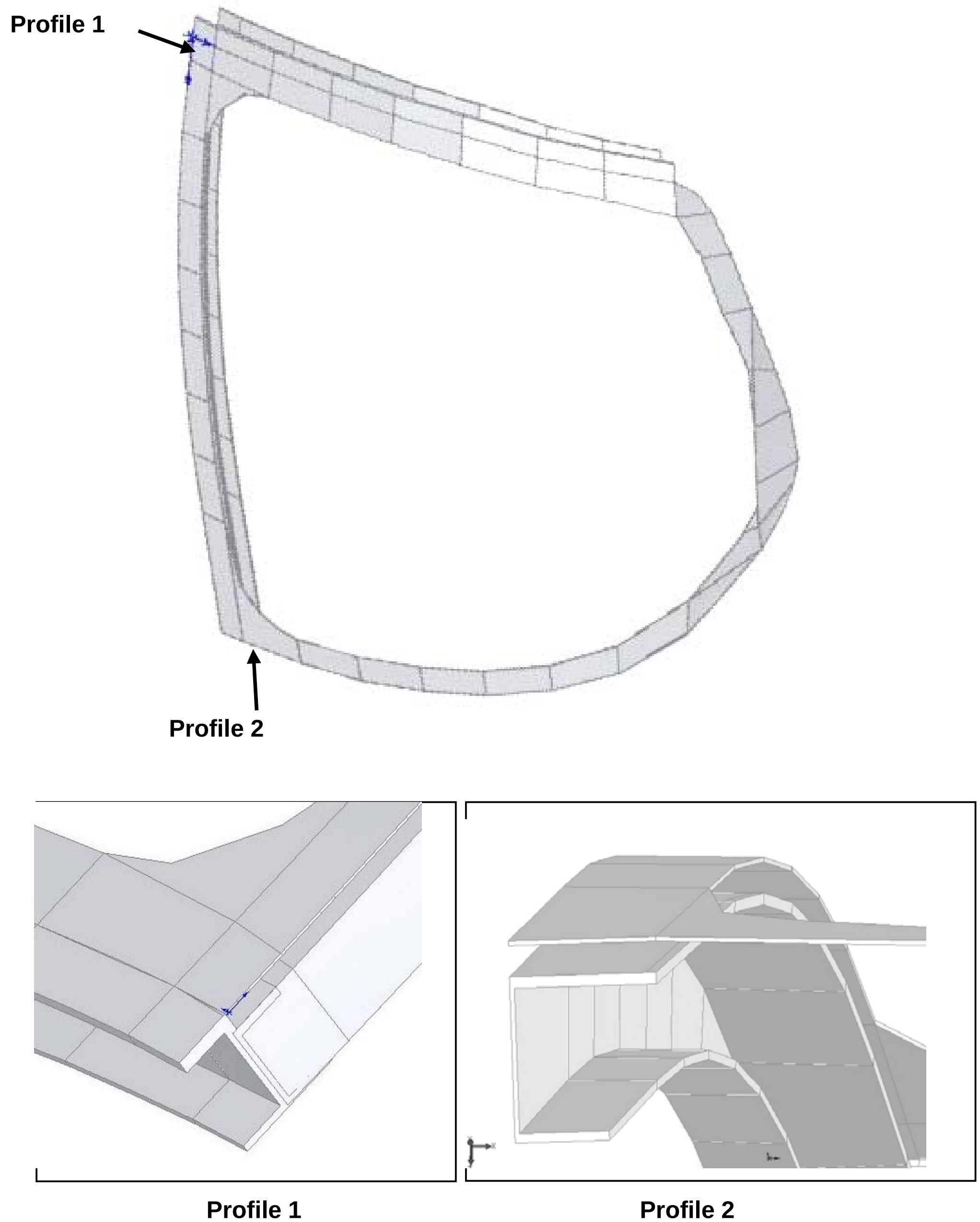

Figure 3 – Plate geometry including the different profiles obtained by the SOLIDWORKS drawing program.

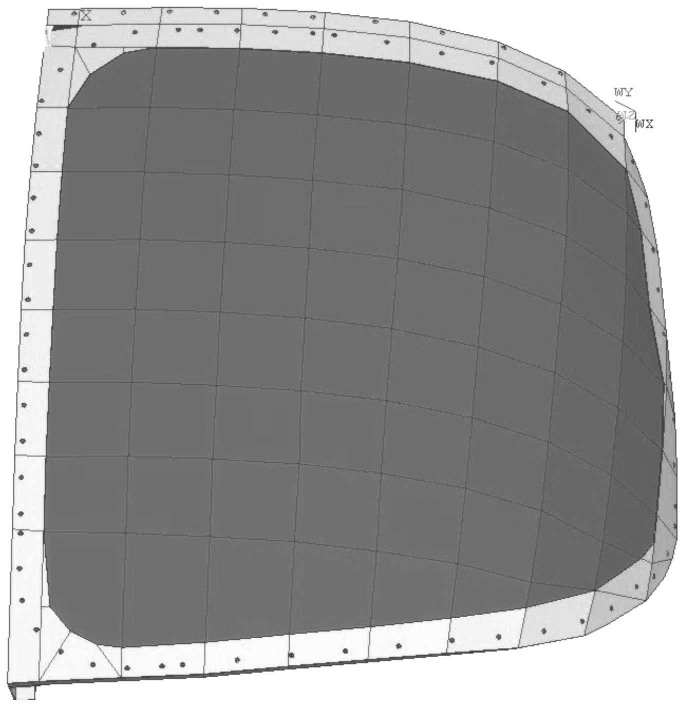

Figure 4 – Set draw reconstruct in the ANSYS Finite Element program.

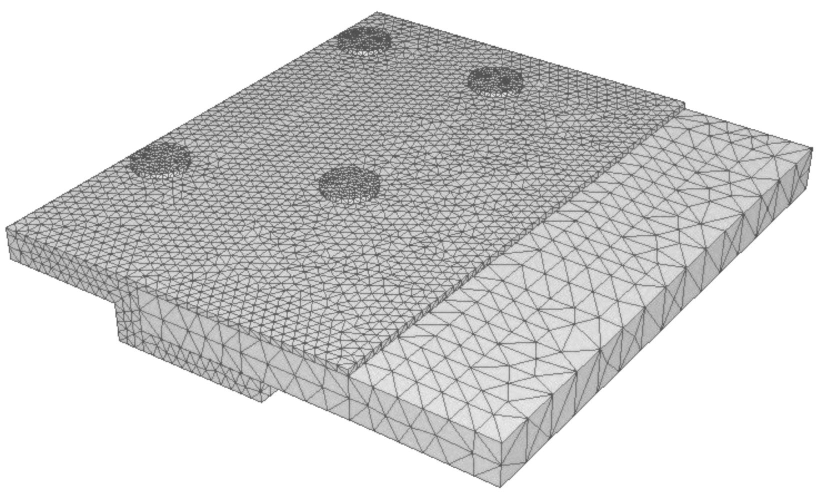

Figure 5 – Specimen meshes.

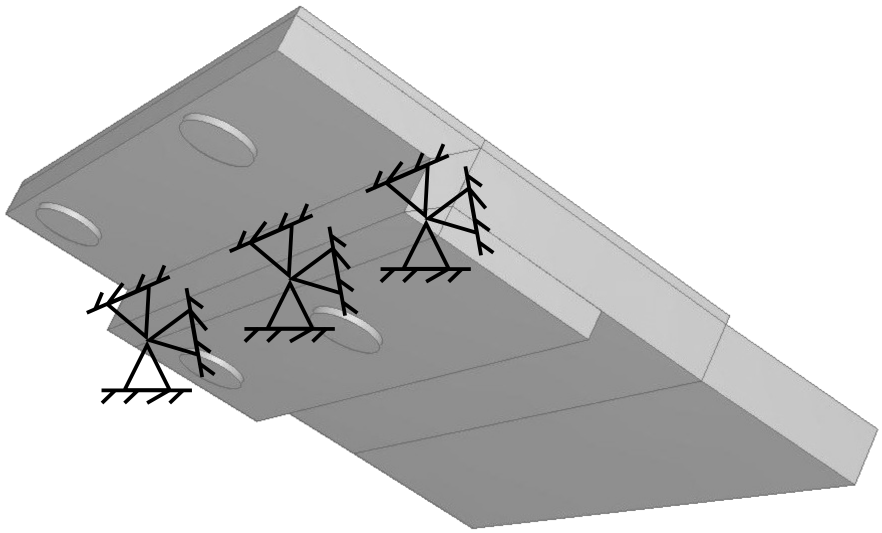

Figure 6 – Boundary conditions applied to the specimen geometry.

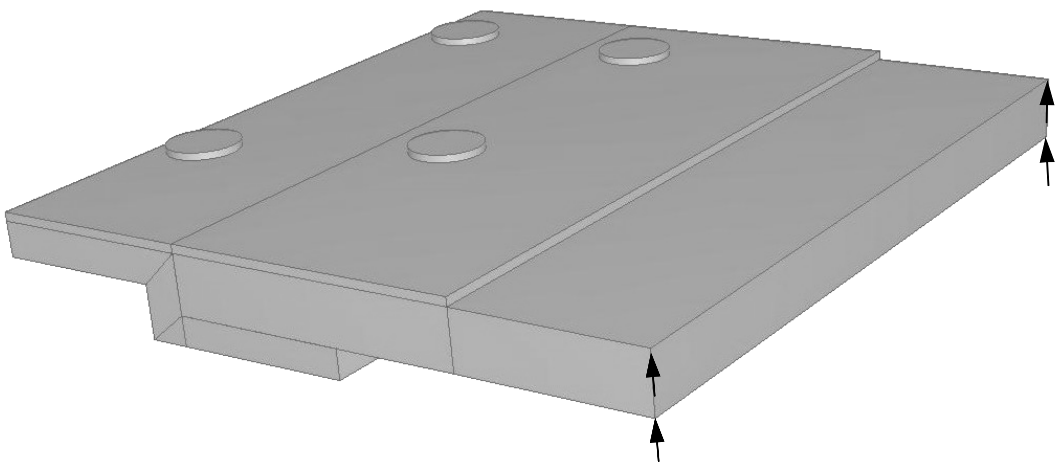

Figure 7 – Load conditions applied to the specimen geometry.

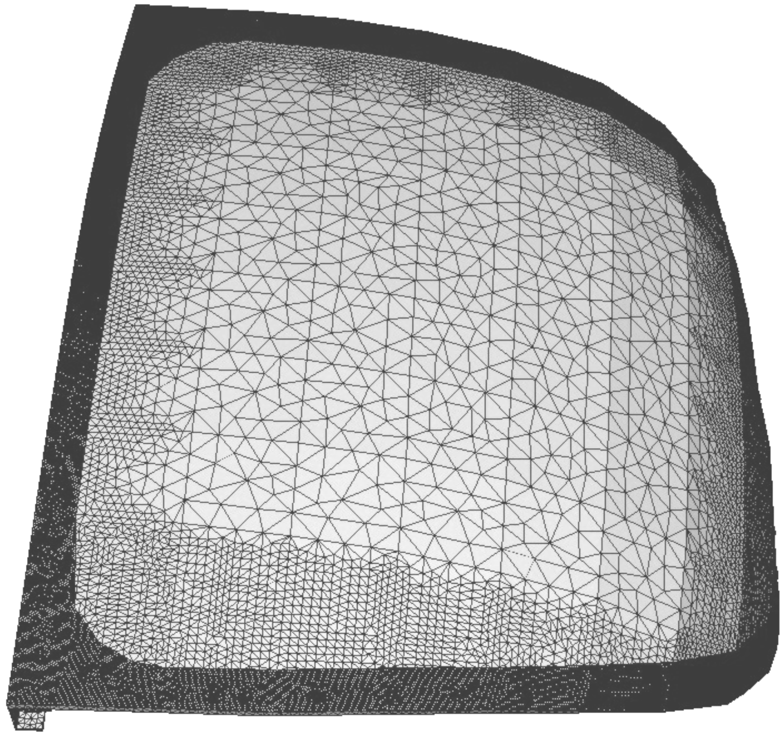

Figure 8 – General view of the cockpit meshes.

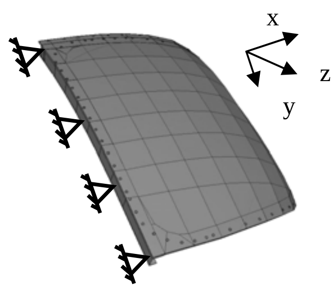	u displacement in x direction applied to the plate and U profile zone
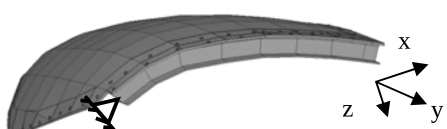	u displacement in x direction applied to the I profile end zone
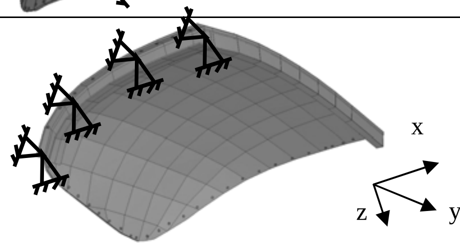	v and w displacements in y and z directions applied to the superior I profile zone

<table>
<tr><td>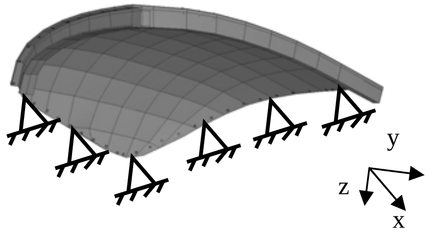</td><td>w displacement in z direction applied to the bolts nuts</td></tr>
<tr><td>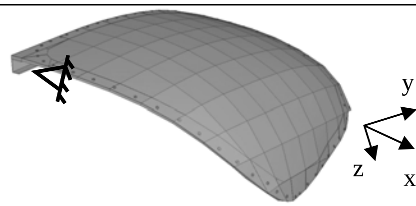</td><td>v and w displacements in y and z directions applied to the U profile center</td></tr>
</table>

Figure 9 - Boundary conditions applied to cockpit geometry

<table>
<tr><td>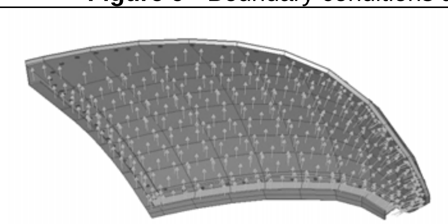</td><td>Axial uniform distribute pressure applied in the interior cockpit zone</td></tr>
<tr><td>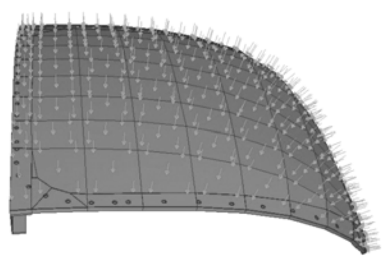</td><td>Axial uniform distribute pressure applied in the external cockpit zone</td></tr>
<tr><td>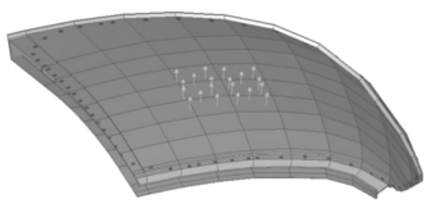</td><td>Axial uniform distribute pressure applied in 4 acrylic glass elements located in the central cockpit zone</td></tr>
<tr><td>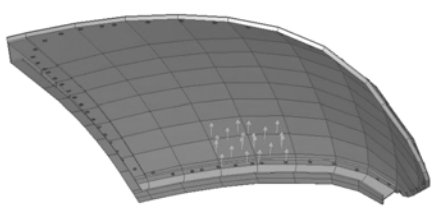</td><td>Axial uniform distribute pressure applied in 4 acrylic glass elements located in the superior cockpit zone</td></tr>
</table>

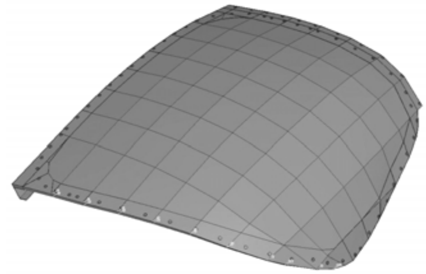	Concentrated loads applied in cockpit inferior edge

Figure 10 - Load condition applied to cockpit geometry

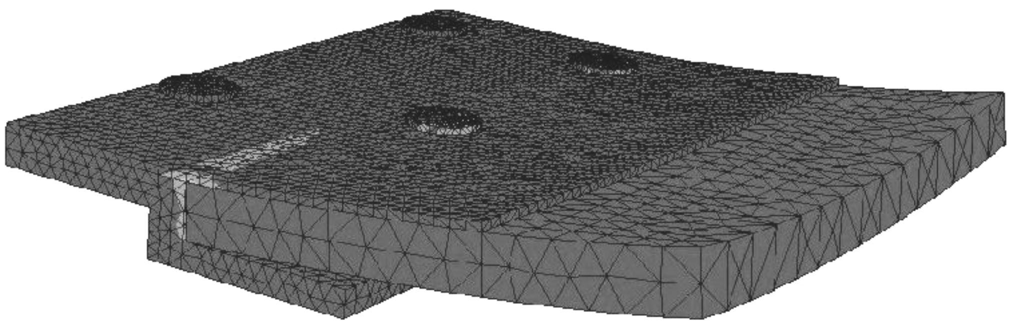

Figure 11 – Mesh deformation obtained in specimen simulation.

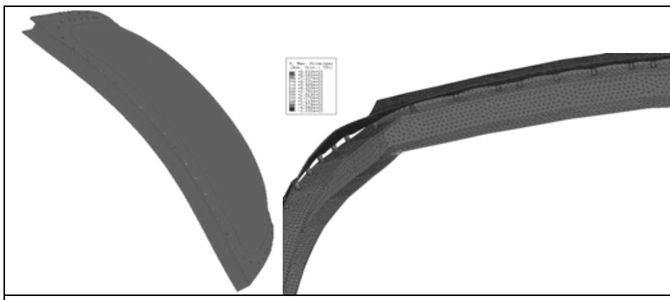	a) Uniform interior pressure was applied. Acrylic glass, plate and aluminum profiles set and bolts and detailed mesh deformation of the set without considered the acrylic glass
	b) Uniform external pressure was applied

	c) Uniform internal pressure was applied in the central cockpit zone
	d) Uniform internal pressure was applied in the superior cockpit zone
	e) Concentrated loads were applied in the inferior cockpit edge

Figure 12 – Mesh deformation obtained in cockpit simulation.